



Molecular evaluation of the prophylactic effect of marine sponge (*Hyrtios sp.*) extract on 1, 2 dimethylhydrazine-induced hepatotoxicity in male rats

Sobhy E. Hasab Elnaby¹, Gihan M. Elkhoudary², Moustafa M. Elmoahalawy², Khaled Y Abdel-Halim³, EL-Hassan M. Mokhamer^{2,*}

¹Zoology Department, Faculty of Science, Menoufia University, Egypt

²Zoology Department, Faculty of Science, Damanhur University, Egypt

³Mammalian and Aquatic Toxicology Department, Central Agricultural Pesticides Laboratory (CAPL), Agricultural Research Center (ARC), Egypt

ARTICLE INFO

Received: 20/12/2025

Revised : 22/1/2025

Accepted: 7/2/2025

Corresponding author:

EL-Hassan. M. Mokhamer, Ph. D

E-mail: elhassan.gaber@sci.dmu.edu.eg

Mobile: (+2)01222510555

P-ISSN: 2974-4334

E-ISSN: 2974-4324

DOI: 10.21608/bbj.2025.362941.1093

ABSTRACT

Hepatic necrosis and regenerative hyperplasia are central to hepatotoxicity development; chronic hepatotoxicity playing a vital role in the initiation and persistence of hepatocellular carcinoma. This study evaluated the alleviative effects of chitosan nanoparticles (CNPs) and marine sponge extract bioactive agents (BAAs), individually and in combination, on 1,2-dimethylhydrazine (DMH)-induced hepatotoxicity in a rat model. Five experimental groups are studied here: normal control, DMH-induced hepatotoxicity, DMH/CNPs, DMH/BAAs, and DMH/BAAs-loaded CNPs. Hepatotoxicity was assessed through immunohistochemical examination of caspase 3 (CASP3), western blot analysis of CASP3 and P27 expressions, and qRT-PCR analysis of *Ctnnb1* and *Ccnd1* gene expressions. DMH administration resulted in severe hepatocellular damage, characterized by elevated CASP3 and decreased P27 levels, and upregulation of *Ctnnb1* and *Ccnd1* gene expression. CNPs or BAAs treatment reduced CASP3, elevated P27 expression, and downregulated *Ctnnb1* and *Ccnd1* gene expression. The most pronounced recovery was observed in the BAAs-loaded CNPs group, where synergistic effects of the combined treatment normalized apoptotic markers, and suppressed WNT/CTNNB signaling. These findings demonstrate that CNPs and BAAs exert hepatoprotective effects by modulating oxidative stress, apoptosis, and cell cycle regulation, with combination therapy offering the greatest protective potential. This study highlights the promise of natural compounds in mitigating a chemical-induced hepatotoxicity and provides a foundation for further research into their mechanisms and clinical applications.

Keywords: Apoptosis, Caspase 3, Gene expression, Hepatotoxicity, P27

1. Introduction

Hepatocellular carcinoma (HCC) is the sixth most common malignant tumor worldwide and a significant cause of cancer-related mortality. Chronic hepatitis B and C virus infections are the primary causes of HCC. These infections cause hepatocellular necrosis and regenerative hyperplasia, which lead to the development of HCC (Fattovich et al., 2004). Other contributing factors include chronic consumption of aflatoxin

B1, alcohol exposure, occupational exposure in rubber and polyester industries, and long-term use of oral contraceptives (Ledda et al., 2017). Advanced hepatic fibrosis (stage F3) is also a significant risk factor (Fujiwara et al., 2018). Hepatocellular necrosis and regenerative hyperplasia are central to hepatotoxicity and chronic hepatotoxicity playing a vital role in the initiation and persistence of HCC (Russo et al.,

2022). Hepatotoxicity may arise from many harmful agents, encompassing pharmaceutical substances, over-the-counter medications, organic solvents, heavy metals, certain therapeutic formulations, and environmental contaminants. Numerous chemical agents capable of provoking hepatotoxicity exert their adverse effects by producing hepatotoxic reactive intermediates. This phenomenon may result from the compound's metabolic activation or the metabolic conversion of a harmless compound into reactive intermediates capable of causing damage to liver cells (Jaeschke & Ramachandran, 2024). In tobacco, specific mushrooms, and certain food items, 1,2-dimethylhydrazine (DMH) has been identified as a toxic environmental pollutant (Kostelc and Hendry, 1981; Liu et al., 1974). Various animal models have been used to extensively document the potential carcinogenicity of DMH, which exhibits selective toxicity in the colon and rectum (Rosenberg et al., 2009). In animal models, DMH is a potential carcinogen that selectively damages the colon and rectum. Furthermore, following metabolism in the liver, it is a potent hepatocarcinogen that causes oxidative stress, hepatotoxicity, and hepatocellular carcinoma (St Clair et al., 1990). Furthermore, it causes mutations in various genes, including the *Ctnnb* and *Apc* genes, by methylating guanines in DNA using its byproducts, methyl diazonium ion and a reactive carbonium ion (Newell & Heddle, 2004). These genes, which are essential components of the WNT pathway, are among the most profound and well-preserved signaling pathways that are implicated in liver and colon malignancies (Wang et al., 2012).

Treatment modalities for HCC include systemic therapy, ablation, transarterial chemoembolization, surgical interventions (liver transplantation and anatomic resection), and chemotherapy, all of which have been found to have limited efficacy, complications, and adverse effects (Kew, 2014). Consequently, significant efforts have been undertaken to identify excellent therapeutic substances that can enhance HCC overall prognosis by selectively targeting and inhibiting tumor-specific pathways.

Natural marine products have shown encouraging anticancer effects on rare occasions,

with normal cells suffering little to no harm. Scientists have looked into many marine sources for possible cancer treatments, including microflora (fungi, cyanobacteria, actinobacteria, and bacteria), macroalgae (seaweeds), invertebrates, sponges, soft corals, and sea fans (Li, 2019; Ren et al., 2021). The sponge species of the genus *Hyrtios* has the following classification: Kingdom Animalia, Phylum Porifera, Class Demospongiae, Order Dictyoceratida, and Family Thorectidae. These sponges have attracted attention as a significant source of bioactive secondary metabolites. The bioactive natural products of *Hyrtios erectus* have been the subject of extensive research. Notably, a diverse array of indole alkaloids has been identified (Sauleau et al., 2006), β -carboline alkaloids (He et al., 2014), and sesterterpenes (Youssef et al., 2002) isolated from *Hyrtios* sp. Subsequent investigations have disclosed that certain compounds exhibit substantial anticancer properties, and antimicrobial activities (Ashour et al., 2007). Overall, the genus *Hyrtios*, represented by species such as *H. erectus* and *H. reticulatus*, offers remarkable potential as a source of structurally unique compounds with promising biological activities. Marine biologically active compounds can work synergistically with existing therapies, enhancing their effectiveness and reducing the risk of drug resistance (Ebrahimi et al., 2022). Chitosan (CS), a polysaccharide, is produced through the deacetylation of chitin (Sharifi-Rad et al., 2021). CS have been used in biomaterials, tissue engineering, and anticancer, antibacterial, antifungal, and antioxidant agents due to its exceptional biocompatibility (A. Muxika et al., 2017). Certain properties of polysaccharides have been proposed to be attributed to CS several chemical transformations. Modified CS samples, including those that have been subjected to phosphorylation, quaternarization, sulfonation, carboxylation, N-alkylation, and acylation, can serve as materials that respond to stimuli. (thermo-, light-, or pH-sensitive) (Argüelles-Monal et al., 2018). Similarly, chitin has been effectively used in many research studies as one of the supporting materials for drug delivery. While there are numerous reported methods of drug delivery, the use of polymeric carriers has drawn significant attention because of its ability

to improve drug-targeting efficacy and prolong the duration of drug circulation by decreasing urine elimination (Dubashynskaya et al., 2022). The objective of this investigation was to evaluate the possibility of biologically active marine material in preventing the development of hepatotoxicity induced by DMH.

2. Materials and methods

Chemicals and reagents

Sigma-Aldrich (St. Louis, MO, USA) was the source of the following materials and compounds: trisodium citrate, methyl red, bromthymol blue, phenolphthalein A, and hemoxilin-eosin (HE). 1,2-Dimethyl hydrazine (DMH, 99% purity) was also acquired from Sigma-Aldrich. Methanol, acetonitrile, polyethylene glycol (PEG), EDTA, formalin, toluene, paraffin, xylene, ethanol, and hydrogen peroxide (H₂O₂) were supplied by BDH Laboratory Supplies (U) Ltd (Kampala, Uganda). Polyclonal antibodies for specific proteins and horseradish peroxidase (HRP) were obtained from Thermo Scientific Co. (USA). Chitosan Nanoparticles (CNPs) suspended in 1% acetic acid solution were provided by Naka Authority (Cairo, Egypt). All primers were procured from Macrogen (Seoul, Republic of Korea). Every other chemical reagent that was employed was of excellent analytical and commercial quality.

Sampling and extraction of bioactive agents (BAAs) of marine sponge

The marine sponges were collected via SCUBA diving from various Red Sea locations near Hurghada, Egypt, in May 2023. Taxonomic identification as *Hyrtios* sp. was conducted by Prof. Gihan EL-Khoudary (Damanhur University) based on morphological characteristics, including skeletal structures (spicules), following the System Porifera classification. After cleaning, the sponges were transported to the lab in an ice box and froze. A portion was cut into small pieces, air-dried in a dark area, and then pulverized. The dried sponge was soaked in 5% w/v methanol overnight, filtered, and rotary-evaporated to dryness; the crude extract was lyophilized and the resulting powder was stored at -30°C until further use (Koopmans et al., 2009).

Animal husbandry and acclimatization

Healthy male Sprague Dewaly rats weighing an average of 100±10 g were provided by the Egyptian Holding Company for Biological Products and Vaccines (VACCERA), Helwan-Egypt. Animals were acclimatized to the environment at the Department of Zoology's animal facility, Faculty of Science, Damanhur University, Egypt, for a week prior to the experiment. The Institutional Animal Care and Use Committee authorized the experimental investigation under the reference number DMU-SCI-CSRE-23-01-04. On an ad libitum basis, the animals were provided with tap water and a standard rodent diet.

Experimental design

Thirty-five animals were divided into five groups, each including seven rats. Group 1 (Gp1) was designated as the negative control and was administered saline via intraperitoneal injection for a period of 12 weeks (wks). Intraperitoneal DMH (20 mg/kg b.w.) was administered once weekly to Gp2, the positive control, for a period of 12 wks (Shebbo et al., 2020). Gp3 received DMH at the same dose as Gp2 along with CNPs (100 mg/kg b.w, orally/once/wk) for the same period (Elsonbaty et al., 2019). Gp4 received DMH alongside BAAs (100 mg/kg b.w, orally/once/wk) for the same duration (Abd El-Moneam et al., 2017). DMH with BAAs-loaded CNPs (100 mg/kg b.w, orally) was administered to Gp5 for the same duration. Rats were given xylazine (10 mg/kg) and ketamine (90 mg/kg) to induce anesthesia before being sacrificed via cervical decapitation 24 hours after the final BAAs treatment at the end of the experiment. Furthermore, they were fastened overnight. As needed, samples were collected for additional analysis

Gas chromatography-mass spectrometry (GC-MS) analysis of BAAs

The analysis used a Thermo Scientific Trace 1300 GC system with a TSQ 9000 mass spectrometer and a TG-5 ms column. The sample, dissolved in acetonitrile, was injected with helium as the carrier gas (1.2 mL/min, splitless mode). The GC temperature program ranged from 40°C to 320°C with specific holds and the mass spectrometer operated in electron impact mode (50 eV, 50–500 m/z). Peaks were

identified using Wiley and NIST libraries (Wallace & Moorthy, 2023).

Preparing of the chitosan nanoparticles linked to marine sponge extract

According to the method of (Calvo et al., 1997), a covalent cross-linkage method was used. Briefly, 100 mg of BAAs were dissolved in 1 ml of methanol. Separately, 9 ml of CNPs were mixed with 0.01 g of PEG and shaken for one hour. The BAAs solution was gradually added to the CNPs suspension, followed by five drops of trisodium citrate, and shaken for 4 hours. The synthesized nanocomposite was then characterized.

Nano-composite characterization

Transmission electron microscope

The prepared nano-polymer, CNPs-linked BAAs was analyzed using transmission electron microscope (TEM; JOEL 1400 Plus, Japan) at 80 kV to determine its morphology and structure. After the NPs were gently agitated, a sample aliquot was sonicated, deposited on a film grid, desiccated, and stained with 1% lead acetate for observation (Bhatt & Madhav, 2011). In order to achieve optimal visualization, bright-field imaging at high magnification was employed in conjunction with diffraction modes.

Droplet size and zeta potential

At room temperature, the prepared CNPs were evaluated for droplet size and zeta potential using a Zeta sizer Nano ZS (Malvern Instruments, UK). The mean particle size was determined through dynamic light scattering (DLS), and the results were presented as the average of three measurements in nanometers. The zeta potential was determined through the use of the light scattering method (Silva et al., 2012). In order to mitigate the possibility of multiple scattering effects, the CNPs solution was diluted 100-fold with distilled water and sonicated for 5 minutes at a pulse rate of 9 cycles/s and 75% power prior to measurement.

Fourier transform infrared (FTIR) spectroscopy

The prepared CNPs were determined using the FTIR instrument (TENSOR 27 Bucker, Germany-FTIR L203/1 2887). The observation was conducted within the 4000 to 400 cm^{-1}

range, with a sensitivity range of 50 and an absolute threshold level of 6.00.

Gene expression of *Ctnnb1* and *Ccnd1*

RNA extraction from liver tissue

The manufacturer's protocol was followed to extract total RNA from liver homogenates using the EasyPure® RNA Kit (TransGen Biotech, Beijing, China). Briefly, 10 mg of liver tissue homogenate was treated with proteinase K, incubated at 56°C, and subsequently centrifuged. The supernatant was mixed with 70% ethanol, transferred to spin columns, and centrifuged to bind RNA. Contaminants were removed using a washing buffer, and DNase I was added to eliminate genomic DNA. After additional washing, RNA was eluted with RNase-free water. The 260/280 ratio and absorbance at 260 nm were used to measure the concentration and purity of RNA, respectively.

cDNA synthesis using RT-PCR

The RevertAid First Strand cDNA Synthesis Kit (Kit #K1622) from Thermo Scientific was employed to produce cDNA from RNA. To conclude, a total volume of 12 μl was achieved by mixing RNA samples (0.1–5 μg) with oligo(dT) primer (1 μl) and nuclease-free water. In the following order: 5 \times reaction buffer (4 μl), RiboLock RNase inhibitor (1 μl , 20 U/ μl), 10 mM dNTP mix (1 μl), and RevertAid M-MuLV RT (2 μl , 200 U/ μl) were added. The cDNA synthesis was completed by delicately combining the mixture, momentarily centrifuging it, and incubating it at 42°C for 60 minutes. Ultimately, the reaction was terminated after being elevated to 70°C for about five minutes. To guarantee its future utilization, the synthesized cDNA was stored at –80°C.

Quantification of *Ctnnb1* and *Ccnd1* gene expression by RT-PCR

The Maxima SYBR Green PCR Kit from Thermo Scientific was employed to quantify the expression of the *Ctnnb1* and *Ccnd1* genes. The reaction mixture (25 μl) contained 12.5 μl of 2 \times SYBR Green master mix, 0.5 μl (0.3 μM) of each primer, 3 μl of cDNA, and 8.5 μl of nuclease-free water. Following a 10-minute initial denaturation at 95°C, the PCR was conducted with 40 cycles of 15 seconds at 95°C, 30 seconds at 60°C, and 30 seconds at 72°C. Primer sequences and

product sizes are listed in Table (1). Utilizing *Actb* as the reference gene, the relative gene expression was determined using the $2^{-\Delta\Delta Ct}$ method. By subtracting the Ct of *Actb* from the Ct of the target gene, the ΔCt value was determined (Yuan et al., 2006).

Western blot analysis of liver tissue proteins

Triton X-100 was employed to lyse the cells after the liver tissues were homogenized in acid and buffer to form pellets. Proteins were separated using SDS-PAGE after the homogenate was prepared in a loading buffer. In order to facilitate western blot analysis, the separated proteins were transferred to a membrane. ACTB (Cat No. MA5-42946), P27 (Cat No. PA5-52634), and active CASP3 (Cat No. PA5-11468) were identified using primary polyclonal antibodies specific for rats. They were then treated with secondary antibodies coupled with horseradish peroxidase. Molecular mass markers (Puregene Protein Ladder, Genetix Biotech) were used as a reference. For protein detection, a Pierce Electro-Chemi-Luminescence (ECL) Western Blotting Kit (Thermo Fisher Scientific) was implemented. The relative densities of protein bands were quantified using the ChemiDoc Imaging System (Bio-Rad).

Immunohistochemical investigation of CASP3 expression

To identify active CASP3 expression in formalin-fixed, paraffin-embedded tissue sections (4 μ m), immunohistochemical (IHC) analysis was implemented employing the peroxidase technique (Petrosyan et al., 2002). H_2O_2 (0.3%) was used to inhibit endogenous peroxidase following deparaffinization, rehydration, and antigen retrieval. Sections were incubated with blocking serum, followed by primary polyclonal antibodies specific for rat active CASP3 (Cat No. PA5-11468), (1:150, Thermo Scientific) overnight, and HRP-conjugated secondary antibody for 15 minutes. Color development was achieved using a peroxidase substrate. Immunoreactivity was quantified using ImageJ software, with the percentage of stained area calculated as: (IHC stained area / total area) \times 100. Nine random fields per slide were analyzed.

Statistical analysis

A one-way ANOVA was implemented, followed by the Tukey *post-hoc* test, to conduct statistical analysis. Statistical significance was determined at $p < 0.05$, and graphs were generated with the GraphPad Prism software. Significance levels were marked as **** for $p < 0.0001$, *** for $p < 0.001$, ** for $p < 0.01$, and * for $p < 0.05$.

3. Results

Bioactive Agents of the Extract (BAAs) as measured by GC-MS

The chromatogram analysis (Fig. 1) identified the bioactive compounds with specific retention times (RT) and biological activities. Key peaks included Cubenol: RT 24.33 min (antioxidant and antimicrobial) (Solís et al., 2004), resibufogenin: RT 34.97 min (antitumor) (Zhou et al., 2022), retinol: RT 36.31 min (antioxidant and anticancer) (Jin et al., 2022), fenretinide: RT 40.09 min (anticancer) (Mody & McIlroy, 2014), and 1,4-benzo-quinone: RT 45.67 min (anticancer) (Ciftci et al., 2022). These results highlight compounds with diverse activities, such as antimicrobial, antifungal, antioxidant, anti-inflammatory, and anticancer properties.

Characterization of chitosan–bioactive sponge extract nanoparticles

Table 2 and Fig 2 demonstrate the average dimension of the chitosan nanoparticles that were prepared was 49.6 ± 11 nm. In contrast, the extract-loaded nanoparticles have an average size of 141.9 ± 14.4 nm, and have a polydispersity value of 0.11. +114.0 mV was determined to be the positive zeta potential of our formulation.

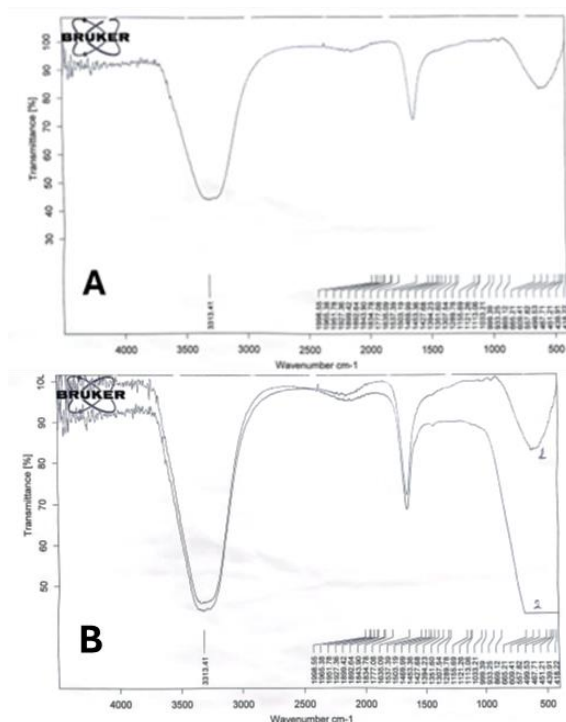


Fig. 3. FTIR profile of (A) CNPs, and (B) CNPs overlapping with BAAs-ligand on CNPs visualized at vibration wavelength at the range 4000 - 400 cm^{-1} .

Gene expression of *Ctnnb1* and *Ccnd1*

Significant changes in the relative expression of *Ctnnb1* (Fig 4A) and *Ccnd1* (Fig 4B) genes were observed across experimental groups in the current study suggesting that CNPs and BAAs have an alleviating effect on DMH-induced hepatotoxicity. In contrast to the normal control, the DMH-induced hepatotoxicity group exhibited a highly significant increase in the expression of *Ctnnb1* and *Ccnd1* genes, indicating the activation of WNT/CTNNB signaling and cell cycle progression, which are associated with hepatotoxicity and potential carcinogenic effects. Conversely, the CNPs treatment exhibited a moderately significant decrease in the expression of both genes in comparison to the positive control group (Gp2), indicating that they may have a protective effect in mitigating DMH-induced hepatotoxicity. A more significant decrease in *Ctnnb1* and *Ccnd1* gene expressions was observed in Gp4, where animals were administered BAAs. This observation underscores the potent antihepatotoxic and antiproliferative effects of the marine sponge BAAs. The synergistic effect of the two treatments in downregulating *Ctnnb1* and *Ccnd1* genes was indicated by the

most considerable decrease in *Ctnnb1* and *Ccnd1* gene expression observed in the marine sponge BAAs loaded CNPs treated group (Gp5). The graphical data presented in Fig. (4) revealed a consistent pattern of declining gene expression from Gp2 through Gp5.

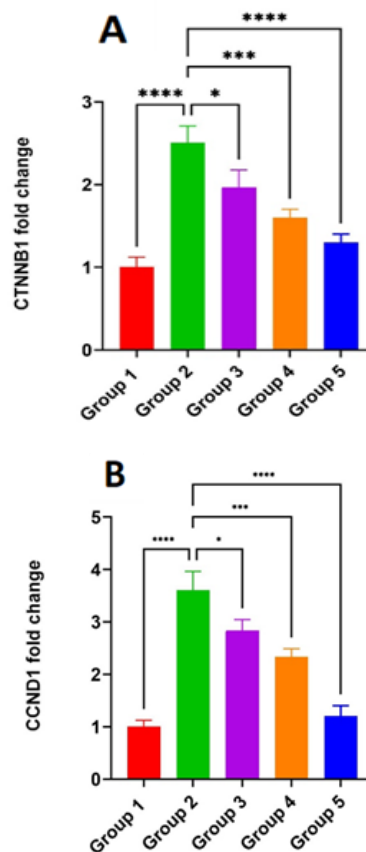


Fig. 4. Relative gene expression (Fold change) of *Ctnnb1* (A), and *Ccnd1* (B) in all studied groups normalized to beta-actin (mean \pm SD).

Western blot analysis of liver tissue proteins

The outcomes of the current research demonstrated significant changes in the relative expression of active CASP3 (Fig 5A) and P27 (Fig 5B), assessed through western blot analysis (Fig 5C), across the experimental groups. These findings underscore the protective effects of CNPs and BAAs against DMH-induced hepatotoxicity. The DMH-induced hepatotoxicity group (Gp2) showed a highly significant increase in CASP3 expression level, while P27 expression was significantly reduced compared to the normal control (Gp1). These alterations indicate increased apoptosis and disrupted cell cycle regulation, which are characteristic of DMH-induced hepatotoxicity. In contrast, the CNPs-

treated group (Gp3) revealed a moderate decrease in CASP3 expression and a moderate increase in P27 levels. A more pronounced improvement was observed in the marine sponge BAAs-treated group (Gp4) where CASP3 expression was significantly decreased, meanwhile, the P27 level was significantly elevated, underscoring the antiapoptotic and cell cycle regulatory effects of the BAAs. In contrast to the positive control group, Gp5 exhibited a highly significant elevated CASP3 expression level alongside a reduced P27 expression, indicating the synergistic protective effect against DMH-induced liver toxicity.

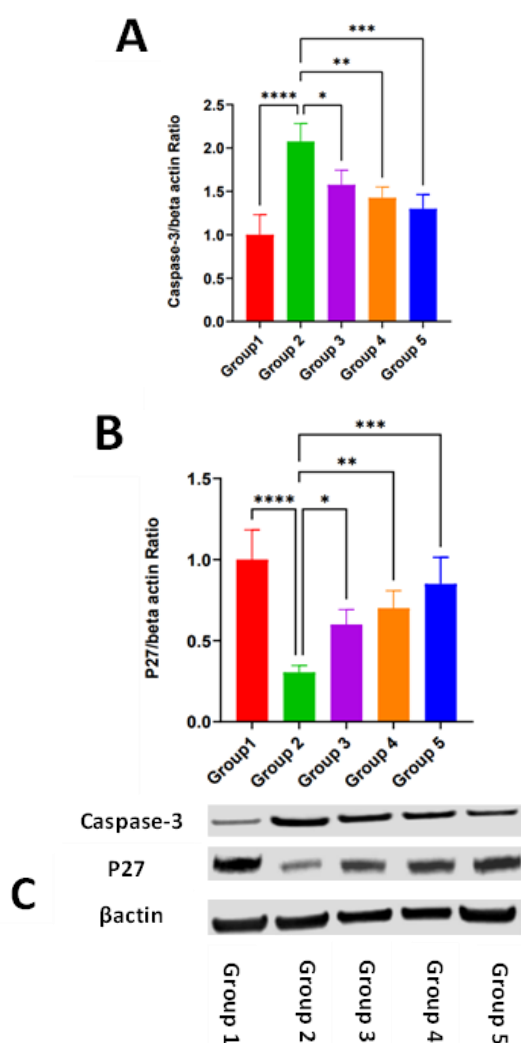


Fig. 5. Effect of CNPs and BAAs on the CASP3 and P27 protein expression in all studied groups normalized to beta-actin, values are expressed mean ±SD

The immunohistochemical analysis

The immunohistochemical analysis of CASP3 expression corroborated the western blot results, providing further evidence of the ameliorative effects of CNPs and BAAs on DMH-induced hepatotoxicity across the five experimental groups. The positive control group exhibited a significant increase in CASP3 immunoreactivity (Fig 6B and Fig 7) compared to the negative control group (Fig 6A and Fig 7), indicating heightened apoptosis due to DMH-induced cellular damage. Meanwhile, CNPs treatment resulted in a moderate reduction in CASP3 expression (Fig 6C and Fig 7), demonstrating their protective role in mitigating apoptosis. A more pronounced decrease in Casp3 immunoreactivity was observed in the BAAs-treated group (Fig 6D and Fig 7), highlighting the potent antiapoptotic properties of the marine sponge extract. The most significant reduction in CASP3 expression was observed in the BAAs-loaded CNPs treated group, confirming the synergistic effect in suppressing apoptosis (Fig 6E and Fig 7).

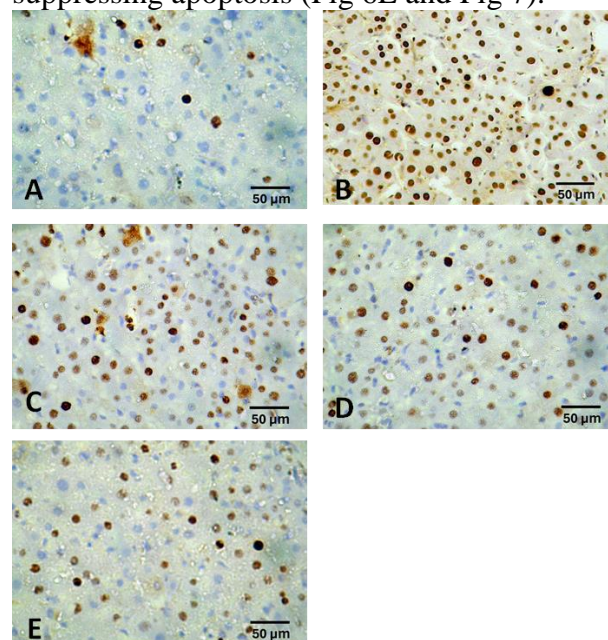


Fig. 6. Caspase 3 immunohistochemical staining of liver tissue in experimental groups. Negative control group (A), positive control group (B), CNPs treated group (C), BAAs-treated group (D), BAAs- loaded CNPs group (E).

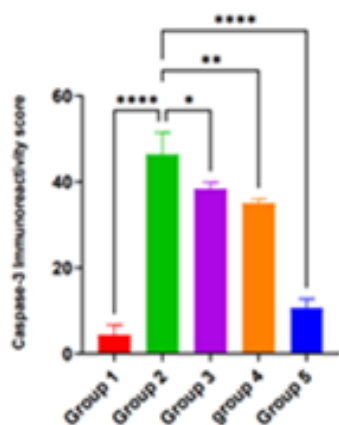


Fig. 7. CASP3 score in the hepatic tissues of different studied groups. Data expressed as Mean \pm SD.

4. Discussion

It is well recognized that reducing the size of nanoparticles in a formulation increases the active medicinal compounds' solubility, bioavailability, and effectiveness (Koukaras et al., 2012). As shown in Fig. (2) and Table (2) the particle size of the extract-loaded chitosan nanoparticles exhibited a difference in particle size from the extract-non-loaded nanoparticles. The polydispersity index indicates the nanoparticle size distribution. It appears to be monodispersed, as our formulation has a polydispersity value of 0.11. The cationic properties of the chitosan nano molecule are correlated with the positive zeta potential of chitosan nanoparticles. This property enables the drug to adhere more effectively to the negatively charged cell membrane, thereby improving drug delivery (Cho et al., 2010). Increased zeta potential magnitude leads to a higher electrostatic repulsion between particles, therefore enhancing the colloidal dispersion's stability. As shown in Table (2), +114.0 mV was determined to be the positive zeta potential of our formulation. It was determined that our formulation was exceptional in light of all of the aforementioned parameters. As a consequence, it was selected for investigation because of its anti-inflammatory and antioxidant defensive potentials. Using the FTIR analysis of CNPs, a broad peak at 3313.41 cm^{-1} was observed, corresponding to the stretching vibrations of $-\text{NH}_2$ and $-\text{OH}$ groups, indicating strong hydrogen bonding. A

peak at 1469 cm^{-1} confirmed the presence of the CONH_2 group in chitosan. Upon loading with BAAs, additional peaks appeared, including a notable absorption at 451.21 cm^{-1} , attributed to C-H stretching vibrations, and aromatic bands at 1167.69 cm^{-1} and 1199.51 cm^{-1} . These changes in the spectra demonstrate the successful integration of BAAs into the chitosan matrix, highlighting the interaction between the NH_2 groups of CS and the functional groups of the BAAs. This confirms the effective loading of sponge extract onto the chitosan nanoparticles.

The outcomes of this investigation emphasize the protective potential of CNPs and BAAs, both individually and in combination, in reducing DMH-induced hepatotoxicity. We elucidated the mechanisms behind these effects by evaluating key molecular markers, such as CASP3, P27, *Ctnnb1*, and *Ccnd1*, using Western blot analysis, immunohistochemistry, and gene expression analysis. In agreement with (Shebbo et al., 2020) the herein results depicted a significant overexpression of *Ctnnb1* in the DMH-induced hepatotoxicity group compared to the normal control group, which is a critical molecular event that contributes to hepatocellular injury and dysregulated cell proliferation. The WNT/CTNNB signaling pathway relies on CTNNB to regulate cell proliferation, survival, and differentiation. In the absence of WNT signaling, the degradation complex that includes adenomatous polyposis coli (APC), axin, and glycogen synthase kinase- 3β (GSK- 3β) is continuously breaking down CTNNB. Moreover, it is indicated that CTNNB is ready for proteasomal degradation and ubiquitination when it is phosphorylated by GSK- 3β (Ding et al., 2005; Zhao et al., 2024). Additionally, the nuclear translocation and stabilization of *Ctnnb* are the effects of DMH exposure, which disrupts this process. This results in the transcriptional activation of target genes, including *Ctnnb1* itself, *Ccnd1* (cyclin D1), and *Myc*, these genes are responsible for hepatocellular injury, impaired apoptosis, and cell proliferation, all of which are typical of DMH-induced hepatotoxicity (Javanmard et al., 2020; Tucker et al., 2003).

In line with recent findings (Shebbo et al., 2020), significant overexpression of *Ccnd1* in the DMH-induced hepatotoxicity group facilitates cell cycle progression via joining cyclin-dependent kinases (CDKs) to generate active complexes, such as CDK4 and CDK6, which phosphorylate and inactivate the retinoblastoma protein (RB) (Calvisi et al., 2007). As a consequence, E2F transcription factors are released, which aid in the transcription of genes that are crucial for the progression of the cell cycle and DNA synthesis (Ren et al., 2002). Furthermore, DMH initiates WNT/CTNNB signaling through the generation of oxidative stress and reactive oxygen species (ROS). ROS impede the phosphorylation and degradation of CTNNB by reducing the activity of GSK-3 β (Son et al., 2013). In addition, the production of pro-inflammatory cytokines, such as TNF- α and IL-6, is increased by DMH-induced inflammation, which in turn activates WNT/CTNNB signaling and contributes to the expression of *Ctnnb1* (Shahbaz et al., 2023). DMH-induced hepatotoxicity may also involve epigenetic modifications that promote *Ctnnb1* overexpression. For example, DNA methylation and histone modifications can alter the transcriptional activity of the *Ctnnb1* gene, leading to its upregulation (Singh et al., 2019).

The Western blot and immunohistochemistry results in the current study confirmed the significant increase of CASP3 expression in Gp2 compared to the control group. These results are in agreement with (Shree et al., 2020), who suggested that DMH induces apoptotic cell death. The intrinsic apoptotic pathway is activated by DMH, which triggers DNA damage and the generation of ROS. This pathway causes the mitochondrial outer membrane (MOMP) to permeabilize and release cytochrome c (Vaish et al., 2013), this initiates the intrinsic apoptotic pathway, where cytochrome c forms the apoptosome with APAF-1 and procaspase-9, resulting in the activation of caspase-9, which subsequently cleaves and activates CASP3 (Saini et al., 2012). In agreement with (Philipp-Staheli et al., 2002), the significant drop in P27 expression in Gp2 can be explained by the

molecular mechanisms of DMH-induced hepatotoxicity, which disrupts cell cycle regulation and promotes uncontrolled cell proliferation. DMH activates the WNT/CTNNB signaling pathway (Sangeetha et al., 2012), which is a key regulator of cell proliferation and survival, as it facilitates the accumulation of CTNNB1 in the cytoplasm and its translocation to the nucleus through this pathway, where, the target genes *Ccnd1* and *Myc* are upregulated as a result of the formation of a complex between Nuclear *Ctnnb1* and TCF/LEF transcription factors. Transcription of *Cdkn1b*, the gene that encodes P27, is directly suppressed by MYC, resulting in a reduction in the level of that protein. Furthermore, P27 is phosphorylated and inactivated by cyclin D1-CDK4/6 complexes, which stimulates its proteasomal degradation (Patel et al., 2008; Tchakarska & Sola, 2020). Moreover, oxidative stress disrupts the stability of P27 by altering its phosphorylation status and promoting its degradation (Jomova et al., 2023).

In agreement with Eslahi et al. (2021) who confirmed the protective impact of CNPs through the inhibition of the WNT/CTNNB1 signaling pathway, our results showed a significant decrease in the expression of *Ctnnb1* and *Ccnd1* in the CNPs-treated group compared to the positive control group. This reduction may be attributed to the modulation of key molecular pathways involved in cell proliferation, apoptosis, and cell cycle regulation. The WNT/CTNNB1 signaling pathway is inhibited by the CNPs, which reduce oxidative stress and prevent the stabilization and nuclear translocation of *Ctnnb1* (Eslahi et al., 2021). Consequently, *Ctnnb1* and its downstream target *Ccnd1* are downregulated, which suppresses uncontrolled cell proliferation (Nasef et al., 2024). Additionally, CNPs showed a moderate decrease in CASP3 expression, this might be due to its antioxidant activity (Anraku et al., 2010; A Muxika et al., 2017), stabilizing mitochondrial membranes, preventing cytochrome c release, and inhibiting the intrinsic apoptotic pathway, while also suppressing NF- κ B signaling to reduce pro-apoptotic gene expression (Bakr et al., 2024).

Consistent with the current results, previous investigations have shown that chitosan and its derivatives influence PI3K-AKT signaling networks, resulting in a dose-dependent decrease in AKT phosphorylation (Xiong et al., 2018). The CNPs demonstrated a significant increase of P27 compared to the positive control group, this may be attributed to its inhibitory effect on the PI3K/AKT/mTOR pathway, preventing P27 phosphorylation and proteasomal degradation, which allows P27 to effectively inhibit cyclin-CDK complexes and promote cell cycle arrest (Amirani et al., 2020). These effects are further augmented by the antioxidant and anti-inflammatory properties of CNPs, which neutralize ROS, reduce DNA damage, and modulate inflammatory cytokines like TNF- α and IL-6. These cytokines are known to promote the expression of *Ctnnb1* and *Ccnd1* genes and suppress P27 (Mohamed et al., 2021).

The present outcomes imply that the significant downregulation of *Ctnnb1* and *Ccnd1* genes in the BAAs-treated group was achieved through a complex web of mechanisms that control cell cycle regulation, apoptosis, and WNT/CTNNB1 signaling. In agreement with (Carroll et al., 2022), who depicted that the administration of sesterterpenoid heteronemin, a bioactive compound of the marine sponge *Hyrtios* extract acts as an antagonist of WNT/CTNNB1 signaling, so the downregulation of *Ctnnb1* and its downstream target *Ccnd1* genes in our study could be caused by the extract's bioactive agents by inhibiting the *Wnt/Ctnnb1* pathway through reducing oxidative stress and preventing β -catenin's nuclear translocation and stabilization. Consequently, uncontrolled cell proliferation was suppressed (Liu et al., 2024). Additionally, the treated group significantly alleviate CASP3 activity by stabilizing mitochondrial membranes, which prevents the release of cytochrome c and inhibits the intrinsic apoptotic pathway. Interestingly, the suppression impact of the marine sponge extract on NF- κ B signaling, led to a reduction in pro-apoptotic gene expression (Choudhary, 2022; Wei et al., 2022). Furthermore, the

marine extract bioactive agents enhance P27 levels by inhibiting the PI3K/AKTmTOR pathway, preventing P27 phosphorylation and proteasomal degradation, which allows P27 to effectively inhibit cyclin-CDK complexes and promote cell cycle arrest (Wei et al., 2020). The antioxidant and anti-inflammatory properties of marine sponge extract BAAs further contribute to these effects by neutralizing ROS, reducing DNA damage, and modulating inflammatory cytokines such as TNF- α and IL-6 which are known to promote *Ctnnb1* and *Ccnd1* expression and suppress p27 (Magri et al., 2023).

The data demonstrated that Gp5, which were treated with marine sponge BAAs loaded CNPs exhibited a highly significant improvement in all measured variables compared to other treatment groups. This suggests a beneficial interactive effect between these two agents. The CNPs acted as an effective delivery system, enhancing the bioavailability (Nagpal et al., 2010) and targeted release of the marine sponge BAAs, which possess potent antioxidant, anti-inflammatory, and antiproliferative properties (Chakraborty & Francis, 2021). Together, these mechanisms synergistically attenuated oxidative stress, alleviated inflammation, and restored hepatic homeostasis, making BAAs-loaded CNPs a highly effective prophylactic strategy for mitigating hepatotoxicity.

Conclusion

According to the current study, marine sponge BAAs are a highly effective prophylactic strategy for mitigating hepatotoxicity, especially when loaded on CNPs as they synergistically attenuate oxidative stress, alleviate inflammation, and restore hepatic homeostasis.

5. Reference

Abd El-Moneam, N. M., Shreadah, M. A., El-Assar, S. A., & Nabil-Adam, A. (2017). Protective role of antioxidants capacity of *Hyrtios* aff. *Erectus* sponge extract against mixture of persistent organic pollutants (POPs)-induced hepatic toxicity in mice liver: biomarkers and ultrastructural study. *Environmental Science and Pollution Research*, 24, 22061-22072.

- Amirani, E., Hallajzadeh, J., Asemi, Z., Mansournia, M. A., & Yousefi, B. (2020). Effects of chitosan and oligochitosans on the phosphatidylinositol 3-kinase-AKT pathway in cancer therapy. *International journal of biological macromolecules*, *164*, 456-467.
- Anraku, M., Michihara, A., Yasufuku, T., Akasaki, K., Tsuchiya, D., Nishio, H., Maruyama, T., Otagiri, M., Maezaki, Y., & Kondo, Y. (2010). The antioxidative and antilipidemic effects of different molecular weight chitosans in metabolic syndrome model rats. *Biological and Pharmaceutical Bulletin*, *33*(12), 1994-1998.
- Argüelles-Monal, W. M., Lizardi-Mendoza, J., Fernández-Quiroz, D., Recillas-Mota, M. T., & Montiel-Herrera, M. (2018). Chitosan Derivatives: Introducing New Functionalities with a Controlled Molecular Architecture for Innovative Materials. *Polymers (Basel)*, *10*(3).
- Ashour, M. A., Elkhayat, E. S., Ebel, R., Edrada, R., & Proksch, P. (2007). Indole alkaloid from the Red Sea sponge *Hyrtios erectus*. *Arkivoc*, *15*, 225-231.
- Bakr, A. F., El-Shiekh, R. A., Mahmoud, M. Y., Khalil, H. M., Alyami, M. H., Alyami, H. S., Galal, O., & Mansour, D. F. (2024). Efficacy of quercetin and quercetin loaded chitosan nanoparticles against cisplatin-induced renal and testicular toxicity via attenuation of oxidative stress, inflammation, and apoptosis. *Pharmaceuticals*, *17*(10), 1384.
- Bhatt, P., & Madhav, S. (2011). A detailed review on nanoemulsion drug delivery system. *International Journal of Pharmaceutical sciences and research*, *2*(10), 2482.
- Calvisi, D. F., Pascale, R. M., & Feo, F. (2007). Dissection of signal transduction pathways as a tool for the development of targeted therapies of hepatocellular carcinoma. *Reviews on recent clinical trials*, *2*(3), 217-236.
- Calvo, P., Remunan-Lopez, C., Vila-Jato, J. L., & Alonso, M. (1997). Novel hydrophilic chitosan-polyethylene oxide nanoparticles as protein carriers. *Journal of applied polymer science*, *63*(1), 125-132.
- Carroll, A. R., Copp, B. R., Davis, R. A., Keyzers, R. A., & Prinsep, M. R. (2022). Marine natural products. *Natural product reports*, *39*(6), 1122-1171.
- Chakraborty, K., & Francis, P. (2021). Apoptotic effect of chromanone derivative, hyrtiosone A from marine demosponge *Hyrtios erectus* in hepatocellular carcinoma HepG2 cells. *Bioorganic Chemistry*, *114*, 105119.
- Cho, Y., Shi, R., & Ben Borgens, R. (2010). Chitosan nanoparticle-based neuronal membrane sealing and neuroprotection following acrolein-induced cell injury. *J Biol Eng*, *4*(1), 2.
- Choudhary, S. (2022). UNVEILING NEGOMBATA MAGNIFICA: A PROMISING FRONTIER IN ANTICANCER RESEARCH. *Annals of Forest Research*, *65*(1).
- Ciftci, H., Sever, B., Kaya, N., Bayrak, N., Yıldız, M., Yıldırım, H., Tateishi, H., Otsuka, M., Fujita, M., & TuYuN, A. F. (2022). Studies on 1, 4-Quinone Derivatives Exhibiting Anti-Leukemic Activity along with Anti-Colorectal and Anti-Breast Cancer Effects. *Molecules*, *28*(1), 77.
- Ding, Q., Xia, W., Liu, J.-C., Yang, J.-Y., Lee, D.-F., Xia, J., Bartholomeusz, G., Li, Y., Pan, Y., & Li, Z. (2005). Erk associates with and primes GSK-3 β for its inactivation resulting in upregulation of β -catenin. *Molecular cell*, *19*(2), 159-170.
- Dubashynskaya, N. V., Petrova, V. A., Romanov, D. P., & Skorik, Y. A. (2022). pH-Sensitive Drug Delivery System Based on Chitin Nanowhiskers-Sodium Alginate Polyelectrolyte Complex. *Materials (Basel)*, *15*(17).
- Ebrahimi, B., Baroutian, S., Li, J., Zhang, B., Ying, T., & Lu, J. (2022). Combination of marine bioactive compounds and extracts for the prevention and treatment of chronic diseases. *Front Nutr*, *9*, 1047026.
- Elsonbaty, S., Moawad, F., & Abdelghaffar, M. (2019). Antioxidants and hepatoprotective effects of chitosan nanoparticles against hepatotoxicity

- induced in rats. *Benha Veterinary Medical Journal*, 36(1), 252-261.
- Eslahi, M., Sadoughi, F., Asemi, Z., Yousefi, B., Mansournia, M. A., & Hallajzadeh, J. (2021). Chitosan and wnt/ β -catenin signaling pathways in different cancers. *Combinatorial Chemistry & High Throughput Screening*, 24(9), 1323-1331.
- Fattovich, G., Stroffolini, T., Zagni, I., & Donato, F. (2004). Hepatocellular carcinoma in cirrhosis: incidence and risk factors. *Gastroenterology*, 127(5), S35-S50.
- Fujiwara, N., Friedman, S. L., Goossens, N., & Hoshida, Y. (2018). Risk factors and prevention of hepatocellular carcinoma in the era of precision medicine. *Journal of Hepatology*, 68(3), 526-549.
- He, W. F., Xue, D. Q., Yao, L. G., Li, J. Y., Li, J., & Guo, Y. W. (2014). Hainanerecramines A-C, alkaloids from the Hainan sponge *Hyrtios erecta*. *Mar Drugs*, 12(7), 3982-3993.
- Jaeschke, H., & Ramachandran, A. (2024). Acetaminophen hepatotoxicity: paradigm for understanding mechanisms of drug-induced liver injury. *Annual Review of Pathology: Mechanisms of Disease*, 19(1), 453-478.
- Javanmard, D., Najafi, M., Babaei, M. R., Karbalaie Niya, M. H., Esghaei, M., Panahi, M., Safarnezhad Tameshkel, F., Tavakoli, A., Jazayeri, S. M., & Ghaffari, H. (2020). Investigation of CTNNB1 gene mutations and expression in hepatocellular carcinoma and cirrhosis in association with hepatitis B virus infection. *Infectious Agents and Cancer*, 15, 1-10.
- Jin, Y., Teh, S. S., Lau, H. L. N., Xiao, J., & Mah, S. H. (2022). Retinoids as anti-cancer agents and their mechanisms of action. *American Journal of Cancer Research*, 12(3), 938.
- Jomova, K., Raptova, R., Alomar, S. Y., Alwasel, S. H., Nepovimova, E., Kuca, K., & Valko, M. (2023). Reactive oxygen species, toxicity, oxidative stress, and antioxidants: Chronic diseases and aging. *Archives of Toxicology*, 97(10), 2499-2574.
- Kew, M. C. (2014). Hepatocellular carcinoma: epidemiology and risk factors. *Journal of hepatocellular carcinoma*, 115-125.
- Koopmans, M., Martens, D., & Wijffels, R. H. (2009). Towards commercial production of sponge medicines. *Mar Drugs*, 7(4), 787-802.
- Kostelc, J. G., & Hendry, L. B. (1981). Hydrocarbon constituents from white strains of the mushroom *Agaricus bisporus* (Lange) Singer. *Journal of agricultural and food chemistry*, 29(1), 185-186.
- Koukaras, E. N., Papadimitriou, S. A., Bikiaris, D. N., & Froudakis, G. E. (2012). Insight on the formation of chitosan nanoparticles through ionotropic gelation with tripolyphosphate. *Mol Pharm*, 9(10), 2856-2862.
- Ledda, C., Loreto, C., Zammit, C., Marconi, A., Fago, L., Matera, S., Costanzo, V., Fuccio Sanzà, G., Palmucci, S., & Ferrante, M. (2017). Non-infective occupational risk factors for hepatocellular carcinoma: A review. *Molecular medicine reports*, 15(2), 511-533.
- Li, Z. (2019). *Symbiotic microbiomes of coral reefs sponges and corals*. Springer.
- Liu, Y.-Y., Schmeltz, I., & Hoffmann, D. (1974). Chemical studies on tobacco smoke. Quantitative analysis of hydrazine in tobacco and cigarette smoke. *Analytical Chemistry*, 46(7), 885-889.
- Liu, Y., Zhou, Z., & Sun, S. (2024). Prospects of marine-derived compounds as potential therapeutic agents for glioma. *Pharmaceutical Biology*, 62(1), 513-526.
- Magri, A. M. P., Avanzi, I. R., Vila, G. T., Granito, R. N., Estadella, D., Jimenez, P. C., Ribeiro, A. M., & Muniz Renná, A. C. (2023). Anti-inflammatory Effects of Compounds Extracted from Marine Sponge s: A Systematic Review. *Anti-Inflammatory & Anti-Allergy Agents in Medicinal Chemistry* (Anti-Inflammatory and Anti-Allergy Agents), 22(3), 164-197.
- Mody, N., & McIlroy, G. D. (2014). The mechanisms of Fenretinide-mediated anti-cancer activity and prevention of obesity and type-2 diabetes. *Biochem Pharmacol*, 91(3), 277-286.
- Mohamed, N. R., Badr, T. M., & Elnagar, M. R. (2021). Efficiency of curcumin and chitosan nanoparticles against toxicity of

- potassium dichromate in male mice. *Int. J. Pharm. Pharm. Sci*, 13, 22159.
- Muxika, A., Etxabide, A., Uranga, J., Guerrero, P., & De La Caba, K. (2017). Chitosan as a bioactive polymer: Processing, properties and applications. *International journal of biological macromolecules*, 105, 1358-1368.
- Muxika, A., Etxabide, A., Uranga, J., Guerrero, P., & de la Caba, K. (2017). Chitosan as a bioactive polymer: Processing, properties and applications. *Int J Biol Macromol*, 105(Pt 2), 1358-1368.
- Nagpal, K., Singh, S. K., & Mishra, D. N. (2010). Chitosan nanoparticles: a promising system in novel drug delivery. *Chemical and Pharmaceutical Bulletin*, 58(11), 1423-1430.
- Nasef, S. M., Mohamed, H. E., & Mansour, S. Z. (2024). Effect of Chitosan-Silver Nanoparticles on DEN-induced Hepatocellular Injury by Regulation of Wnt/ β -Catenin and Apoptosis Signaling Pathways in Rats. *ChemistrySelect*, 9(23), e202400356.
- Newell, L. E., & Heddle, J. A. (2004). The potent colon carcinogen, 1,2-dimethylhydrazine induces mutations primarily in the colon. *Mutat Res*, 564(1), 1-7.
<https://doi.org/10.1016/j.mrgentox.2004.06.005>
- Patel, R., Ingle, A., & Maru, G. B. (2008). Polymeric black tea polyphenols inhibit 1, 2-dimethylhydrazine induced colorectal carcinogenesis by inhibiting cell proliferation via Wnt/ β -catenin pathway. *Toxicology and applied pharmacology*, 227(1), 136-146.
- Petrosyan, K., Tamayo, R., & Joseph, D. (2002). Sensitivity of a novel biotin-free detection reagent (Powervision⁺TM) for immunohistochemistry. *Journal of histotechnology*, 25(4), 247-250.
- Philipp-Staheli, J., Kim, K.-H., Payne, S. R., Gurley, K. E., Liggitt, D., Longton, G., & Kemp, C. J. (2002). Pathway-specific tumor suppression: reduction of p27 accelerates gastrointestinal tumorigenesis in Apc mutant mice, but not in Smad3 mutant mice. *Cancer cell*, 1(4), 355-368.
- Ren, B., Cam, H., Takahashi, Y., Volkert, T., Terragni, J., Young, R. A., & Dynlacht, B. D. (2002). E2F integrates cell cycle progression with DNA repair, replication, and G2/M checkpoints. *Genes & development*, 16(2), 245-256.
- Ren, X., Xie, X., Chen, B., Liu, L., Jiang, C., & Qian, Q. (2021). Marine Natural Products: A Potential Source of Anti-hepatocellular Carcinoma Drugs. *J Med Chem*, 64(12), 7879-7899.
- Rosenberg, D. W., Giardina, C., & Tanaka, T. (2009). Mouse models for the study of colon carcinogenesis. *Carcinogenesis*, 30(2), 183-196.
- Russo, F. P., Zanetto, A., Pinto, E., Battistella, S., Penzo, B., Burra, P., & Farinati, F. (2022). Hepatocellular carcinoma in chronic viral hepatitis: where do we stand? *International Journal of Molecular Sciences*, 23(1), 500.
- Saini, M. K., Sanyal, S. N., & Vaiphei, K. (2012). Piroxicam and C-phycocyanin mediated apoptosis in 1, 2-dimethylhydrazine dihydrochloride induced colon carcinogenesis: exploring the mitochondrial pathway. *Nutrition and cancer*, 64(3), 409-418.
- Sangeetha, N., Viswanathan, P., Balasubramanian, T., & Nalini, N. (2012). Colon cancer chemopreventive efficacy of silibinin through perturbation of xenobiotic metabolizing enzymes in experimental rats. *European journal of pharmacology*, 674(2-3), 430-438.
- Sauleau, P., Martin, M. T., Dau, M. E., Youssef, D. T., & Bourguet-Kondracki, M. L. (2006). Hyrtiazepine, an azepino-indole-type alkaloid from the Red Sea marine sponge *Hyrtios erectus*. *J Nat Prod*, 69(12), 1676-1679.
- Shahbaz, M., Naeem, H., Momal, U., Imran, M., Alsagaby, S. A., Al Abdulmonem, W., Waqar, A. B., El-Ghorab, A. H., Ghoneim, M. M., & Abdelgawad, M. A. (2023). Anticancer and apoptosis inducing potential of quercetin against a wide range of human malignancies. *International Journal of Food Properties*, 26(1), 2590-2626.

- Sharifi-Rad, J., Quispe, C., Butnariu, M., Rotariu, L. S., Sytar, O., Sestito, S., Rapposelli, S., Akram, M., Iqbal, M., Krishna, A., Kumar, N. V. A., Braga, S. S., Cardoso, S. M., Jafarnik, K., Ekiert, H., Cruz-Martins, N., Szopa, A., Villagran, M., Mardones, L., . . . Calina, D. (2021). Chitosan nanoparticles as a promising tool in nanomedicine with particular emphasis on oncological treatment. *Cancer Cell Int*, 21(1), 318.
- Shebbo, S., El Joumaa, M., Kawach, R., & Borjac, J. (2020). Hepatoprotective effect of *Matricaria chamomilla* aqueous extract against 1, 2-Dimethylhydrazine-induced carcinogenic hepatic damage in mice. *Heliyon*, 6(6).
- Shree, A., Islam, J., Vafa, A., Mohammad Afzal, S., & Sultana, S. (2020). Gallic acid prevents 1, 2-Dimethylhydrazine induced colon inflammation, toxicity, mucin depletion, and goblet cell disintegration. *Environmental toxicology*, 35(6), 652-664.
- Silva, A. L., Júnior, F. A., Verissimo, L. M., Agnez-Lima, L. F., Egito, L. C. M., De Oliveira, A. G., & Do Egito, E. S. T. (2012). Physical factors affecting plasmid DNA compaction in stearylamine-containing nanoemulsions intended for gene delivery. *Pharmaceuticals*, 5(6), 643-654.
- Singh, V., Singh, A. P., Sharma, I., Singh, L. C., Sharma, J., Borthakar, B. B., Rai, A. K., Katak, A. C., Kapur, S., & Saxena, S. (2019). Epigenetic deregulations of Wnt/ β -catenin and transforming growth factor beta-Smad pathways in esophageal cancer: Outcome of DNA methylation. *Journal of cancer research and therapeutics*, 15(1), 192-203.
- Solís, C., Becerra, J., Flores, C., Robledo, J., & Silva, M. (2004). Antibacterial and antifungal terpenes from *Pilgerodendron uviferum* (D. Don) Florin. *Journal of the Chilean Chemical Society*, 49(2), 157-161.
- Son, Y.-O., Pratheeshkumar, P., Wang, L., Wang, X., Fan, J., Kim, D.-H., Lee, J.-Y., Zhang, Z., Lee, J.-C., & Shi, X. (2013). Reactive oxygen species mediate Cr (VI)-induced carcinogenesis through PI3K/AKT-dependent activation of GSK-3 β / β -catenin signaling. *Toxicology and applied pharmacology*, 271(2), 239-248.
- St Clair, W. H., Billings, P. C., Carew, J. A., Keller-McGandy, C., Newberne, P., & Kennedy, A. R. (1990). Suppression of dimethylhydrazine-induced carcinogenesis in mice by dietary addition of the Bowman-Birk protease inhibitor. *Cancer Res*, 50(3), 580-586.
- Tchakarska, G., & Sola, B. (2020). The double dealing of cyclin D1. *Cell cycle*, 19(2), 163-178.
- Tucker, E., Buda, A., Janghra, N., Baker, J., Coad, J., Moorghan, M., Havler, M., Dettmar, P., & Pignatelli, M. (2003). Abnormalities of the cadherin-catenin complex in chemically-induced colorectal carcinogenesis. *Proceedings of the Nutrition Society*, 62(1), 229-236.
- Vaish, V., Piplani, H., Rana, C., Vaiphei, K., & Sanyal, S. N. (2013). NSAIDs may regulate EGR-1-mediated induction of reactive oxygen species and non-steroidal anti-inflammatory drug-induced gene (NAG)-1 to initiate intrinsic pathway of apoptosis for the chemoprevention of colorectal cancer. *Molecular and cellular biochemistry*, 378, 47-64.
- Wallace, W. E., & Moorthy, A. S. (2023). NIST Mass Spectrometry Data Center standard reference libraries and software tools: Application to seized drug analysis. *Journal of forensic sciences*, 68(5), 1484-1493.
- Wang, J., Sinha, T., & Wynshaw-Boris, A. (2012). Wnt signaling in mammalian development: lessons from mouse genetics. *Cold Spring Harb Perspect Biol*, 4(5).
- Wei, J., Gou, Z., Wen, Y., Luo, Q., & Huang, Z. (2020). Marine compounds targeting the PI3K/Akt signaling pathway in cancer therapy. *Biomedicine & Pharmacotherapy*, 129, 110484.
- Wei, J., Liu, Y., Teng, F., Li, L., Zhong, S., Luo, H., & Huang, Z. (2022). Anticancer effects of marine compounds blocking the nuclear factor kappa B signaling pathway. *Molecular Biology Reports*, 49(10), 9975-9995.

- Xiong, H., Wu, M., Zou, H., Jiang, S., Yi, H., Yi, T., Wang, Q., Liu, D., Zhou, Y., & Wei, C. (2018). Chitosan inhibits inflammation and adipogenesis of orbital fibroblasts in Graves ophthalmopathy. *Molecular Vision*, *24*, 509.
- Youssef, D. T., Yamaki, R. K., Kelly, M., & Scheuer, P. J. (2002). Salmahyrtilol A, a novel cytotoxic sesterterpene from the Red Sea sponge *Hyrtilos erecta*. *J Nat Prod*, *65*(1), 2-6.
- Yuan, J. S., Reed, A., Chen, F., & Stewart, C. N., Jr. (2006). Statistical analysis of real-time PCR data. *BMC bioinformatics*, *7*, 85.
- Zhao, Z., Cui, T., Wei, F., Zhou, Z., Sun, Y., Gao, C., Xu, X., & Zhang, H. (2024). Wnt/ β -Catenin signaling pathway in hepatocellular carcinoma: pathogenic role and therapeutic target. *Frontiers in oncology*, *14*, 1367364.
- Zhou, Y., Hong, Z., Jin, K., Lin, C., Xiang, J., Ge, H., Zheng, Z., Shen, J., & Deng, S. (2022). Resibufogenin inhibits the malignant characteristics of multiple myeloma cells by blocking the PI3K/Akt signaling pathway. *Experimental and Therapeutic Medicine*, *24*(1), 1-7.